

# Pedestrian Crossing Discrepancy Within Static and Dynamic Crowds: An Experimental Study

JINGHUI WANG,<sup>1</sup> YAJUAN JIANG,<sup>1</sup> XIAOYING ZHANG,<sup>2</sup> FANGWEI DENG,<sup>1</sup> AND WEI LV<sup>1,\*</sup>

<sup>1</sup>*School of Safety Science and Emergency Management  
Wuhan University of Technology  
Wuhan, China*

<sup>2</sup>*Institute of Information Technology  
Hainan Vocational University of Science and Technology  
Haikou, China*

## ABSTRACT

This paper aims to investigate the disparities in pedestrian crossing behaviors within static and dynamic crowds through experimental analysis. First, the crossing trajectories of pedestrians in various crowd environments were qualitatively observed. These trajectories have shown significant discrepancies and the phenomenon of cross-channel formation within static crowds was observed, a phenomenon similar to the evolution of human trails. To quantitatively assess these discrepancies, metrics of behavior patterns and swarm factor were introduced. Different behavioral patterns, including anticipation and reaction behaviors in pedestrian motion, were observed. Finally, through orthogonal velocity analysis, the variation trends of crossing motions within static and dynamic contexts were revealed.

*Keywords:* Crossing behavior, Static and dynamic crowd, Cross-channel formation, Anticipation behavior, Experiment

## 1. INTRODUCTION

The frequent occurrence of crowd crush accidents has significantly impacted public safety, emphasizing the crucial necessity for crowd research (Feliciani et al. 2023). The complicated mechanism of the crowd has caused huge challenges to the relevant investigation. Common forms of cross motion include unidirectional flow (Ma et al. 2015), bidirectional flow (Feliciani & Nishinari 2016), cross-flow (Cao et al. 2017; Zanlungo et al. 2023b), and bottleneck flow (Seyfried et al. 2009), among others. Researchers have conducted classified studies for the investigation of motion patterns, involving the stop-and-go wave (Portz & Seyfried 2011), lane formation (Feliciani & Nishinari 2016), arching phenomenon (Zuriguel et al. 2020), and turbulence (Helbing et al. 2007), to name a few. The typical pedestrian crossing scenario is the crossing flow. The interweaving of mutually perpendicular pedestrian flows gives rise to the stripe phenomenon, a typical self-organizing pattern that helps reduce the "friction" of crossing flows. Subsequently, further pedestrian experiments and the development of models on this topic were conducted (Cao et al. 2017; Zanlungo et al. 2023b; Mullick et al. 2022; Zanlungo et al. 2023a). Beyond these, research on individual pedestrian behavior has also been further explored. Studies have revealed that crowds attempt to avoid longitudinal intrusions by employing lateral motions (Nicolas et al. 2019). And pedestrians have been observed to cross through extremely dense environments successfully. These findings highlight the dynamics of pedestrian motion in dense crowds are hardly expressed by mechanical descriptions (Kleinmeier et al. 2020). An empirical study concerning the "Love Parade Disaster" identified two types of pedestrians within dense crowds: active and inactive (Ma et al. 2015). Active pedestrians persistently create pathways in crowded conditions, while inactive individuals resort to localized movement driven by forces and spatial constraints, analogous to the research presented by (Parisi et al. 2016).

In general, pedestrian crossing behaviors exhibit diverse characteristics and are influenced by social norms. The most frequent motion within crowds is crossing behavior. For instance, in the subway, passengers often cross the crowd toward the exit, and during music festivals, audiences need to cross the crowd to reach the front, among other examples. Although these crossing phenomena are ubiquitous in daily life, but we currently possess limited

\* weil@whut.edu.cn

**Table 1:** Setup for crossing experiment.

Index	Crowd contexts	Geometrical configuration (m <sup>2</sup> )	Crossing distance (m)	No. of participants	Global density (ped/m <sup>2</sup> )	No. of repetitions
S(D)-L5-N0	Static (Dynamic)	5×5	5	0	0	30
S(D)-L5-N5	Static (Dynamic)	5×5	5	5	0.2	50 (39)
S(D)-L5-N10	Static (Dynamic)	5×5	5	10	0.4	50 (39)
S(D)-L5-N15	Static (Dynamic)	5×5	5	15	0.6	49 (39)
S(D)-L5-N20	Static (Dynamic)	5×5	5	20	0.8	50 (40)
S(D)-L5-N25	Static (Dynamic)	5×5	5	25	1	49 (38)
S(D)-L5-N30	Static (Dynamic)	5×5	5	30	1.2	50 (39)
S(D)-L5-N35	Static (Dynamic)	5×5	5	35	1.4	49 (34)
S(D)-L5-N40	Static (Dynamic)	5×5	5	40	1.6	45 (35)
S(D)-L5-N45	Static (Dynamic)	5×5	5	45	1.8	51 (23)
S(D)-L5-N49	Static (Dynamic)	5×5	5	49	1.96	24 (20)
S(D)-L3-N18	Static (Dynamic)	3.8×3.2	3.8	18	1.48	29 (30)
S(D)-L3-N24	Static (Dynamic)	3.8×3.2	3.8	24	1.97	29 (29)
S(D)-L3-N30	Static (Dynamic)	3.8×3.2	3.8	30	2.47	29 (29)
S(D)-L3-N36	Static (Dynamic)	3.8×3.2	3.8	36	2.96	29 (29)
S(D)-L3-N42	Static (Dynamic)	3.8×3.2	3.8	42	3.45	16 (17)

knowledge. A potential reason lies in the significant risks associated with conducting controlled experiments involving dense crowds (Jin et al. 2019). Therefore, to date, related research remains limited. To this end, a series of crowd-crossing experiments are established to conduct a comprehensive analysis of these frequently overlooked behaviors. The structure of this paper is organized as follows: In the next section, we will introduce the experimental setup. In Section 3, the trajectory characteristics of crossing pedestrians will be analyzed. Subsequently, in Section 4, the differential performances of pedestrian motion in static and dynamic contexts will be quantitatively presented and the conclusions are provided in Section 5.

## 2. EXPERIMENTAL SETUP

Experiments were conducted within the campus of Wuhan University of Technology, involving a total of 50 participants with a gender ratio of 1:1. The schematic diagram is presented in Fig. 1. Participants sequentially cross through the experimental area, considering two control conditions: global density and crowd contexts (static or dynamic). In the static context, the participants remained stationary within the experiment area during the crossing process, unable to move freely. Conversely, the dynamic context allowed participants to move freely within the experimental area. The experiment was conducted under both low-density and high-density conditions, with different configurations. The experimental area for the low-density (L5 class) was set at 5 m × 5 m, while the high-density (L3 class) was set at 3.8 m × 3.2 m. To ensure the mitigation of boundary effects, 3/5 of the central area was selected as the designated measurement area. Tab. 1 presents the configuration of the experiments, while Fig. 1 illustrates the scenarios in both static and dynamic experiments. See Wang et al. (2023) for the details related to the experiments and the data processing procedures.

## 3. TRAJECTORY FEATURES

This section explored the discrepancy in crossing trajectories within static and dynamic contexts.

### 3.1. Trajectories

The trajectory of cross pedestrians in each experiment was presented in Fig. 2, and the corresponding experiment index was marked at each subfigure. Within the static context, pedestrians primarily crossing by the fixed channels, referred to as "cross-channel formations", shares the resemblance to the human trail evolution (Helbing et al. 1997; Moussaïd et al. 2009), as illustrated in Fig. 3. Conversely, the trajectories presented more stochastic in the dynamic context.

### 3.2. Cross-channel Formation Mechanism

For the investigation of cross-channel formation, we observed the channel evolution within the local area field. Notably, the local area field, defined as the Thiessen polygon area occupied by individuals (Steffen & Seyfried 2010), was the most intuitive metric of space during the pedestrian crossing process. Fig. 4 illustrates the distribution of the local area field, spanning from experiment S-L5-N10 to experiment S-L5-N49. The orange curve represents the

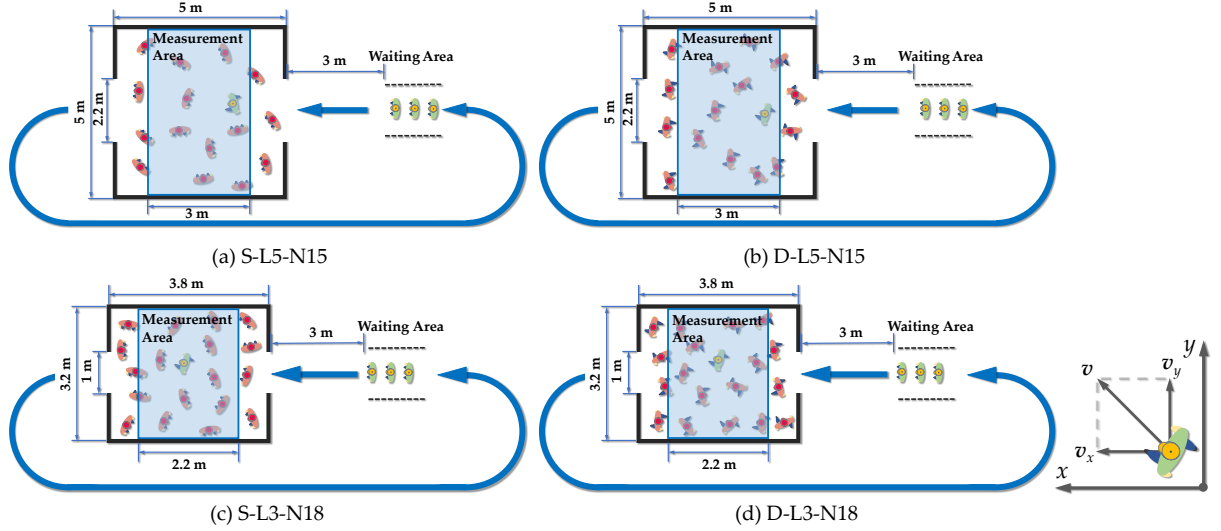


**Figure 1:** Schematic illustration of experimental scenarios.

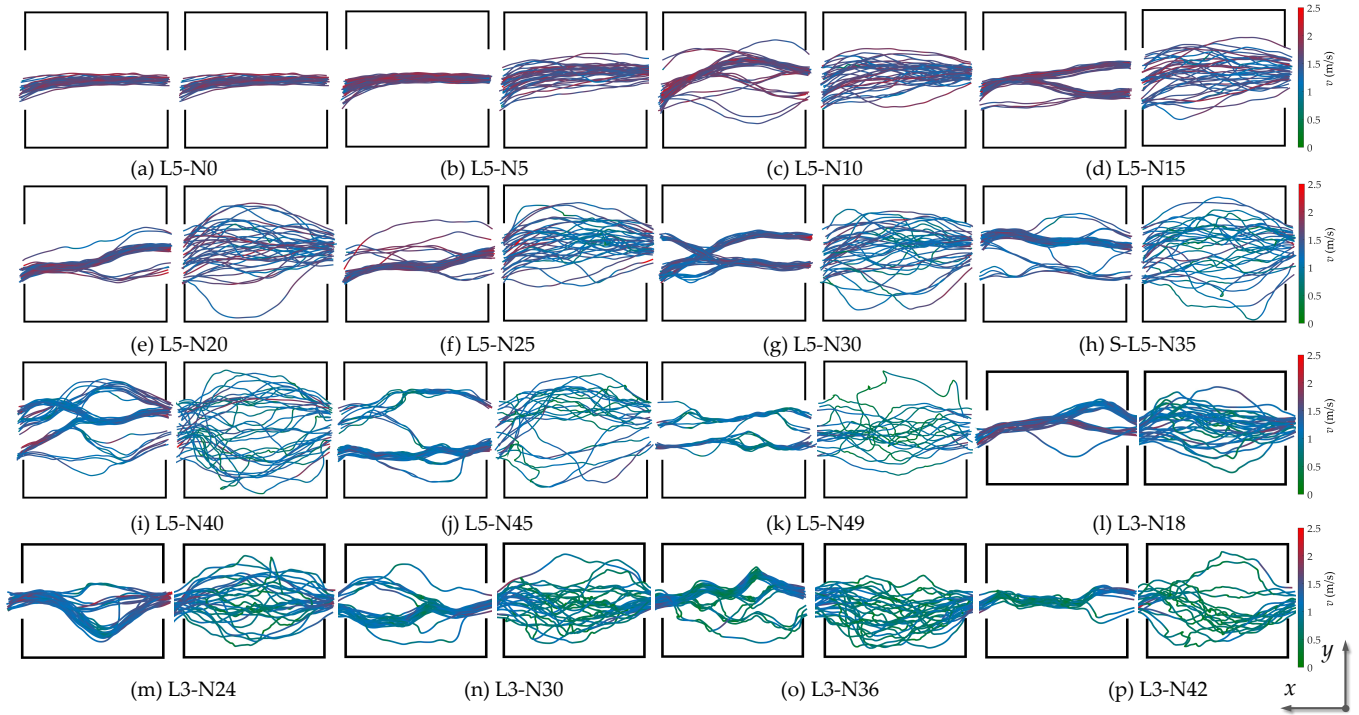


**Figure 2:** Pedestrian trajectory in static and dynamic crowds (on the left side of each subfigure: static experiment, on the right side: dynamic experiment). The positive direction of the  $x$ -axis in the lower right corner of the image indicates the pedestrian's direction of crossing).

trajectory of each pedestrian. Subfigures (a)-(d) presented that pedestrians tend to select the shortest straight route when the density is low, resulting in trajectories without detours. Along with the global density increase, the local area field notably influences pedestrians' trajectories. Pedestrians seem likely to opt for directions with higher local areas when detours are necessary. Despite the diverse mechanisms employed by individuals in selecting their routes, a predominant trend emerges wherein the majority of pedestrians converge upon some particular routes.

In high-density situations, pedestrians frequently make detours to plan their routes. Fig.4(e) presents pedestrians crossing along orientations parallel to the human walls instead of crossing through them. Instead, the human walls

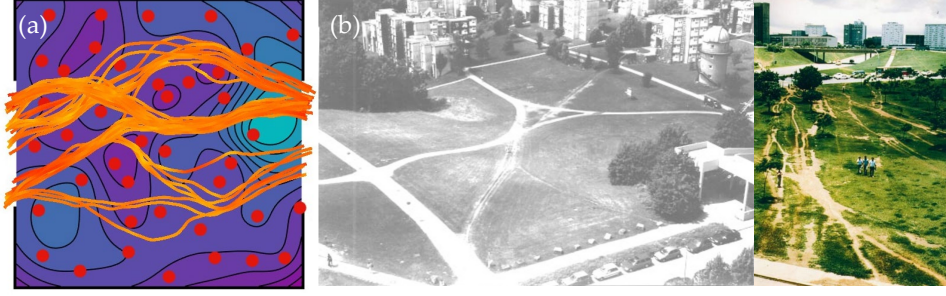


**Figure 3:** (a) Cross-channel formation (experiment index: S-L5-N40) and (b) pedestrian trail evolution in grassland, Source: Helbing et al. (1997).

also will obstruct the crossing route, forcing pedestrians to take wider detours. In the local area field depicted in Fig.4(h), an empty area is present at the entrance (yellow arrow), making it a favorable choice for crossing. However, pedestrians plan their routes around the empty area due to the challenges posed by the two human walls behind it (yellow wavy line). The phenomena imply that, beyond the crossing strategies driven by lower spatial constraints, pedestrians may opt for localized sacrifices to attain wiser strategies on an extensive scale.

## 4. COMPARISONS

The observation mentioned above has qualitatively analyzed the different characteristics of pedestrians crossing. In this section, we conducted a quantitative analysis of pedestrian behavioral patterns and velocity variation.

### 4.1. Behavior Analysis

#### 4.1.1. Definitions

#### Anticipation and Reaction Behavior

To investigate the potential behavior patterns within pedestrian motion, we defined anticipation and reaction behaviors. Anticipation behavior refers to pedestrians proactively adjusting for imminent situations. Correspondingly, reaction behavior refers to the phenomenon where pedestrians, in post-response to imminent situations, are exemplified in the following behavior in single-file motion or the overdamped phenomenon (Cordes et al. 2023), etc, as illustrated in Fig.5.

Anticipation behavior and reaction behavior can be quantitatively classified by the concept of Speed-Space Time Delay (TD) (Wang et al. 2024). In non-free flow motion, the TD ( $\delta$ ) manifested as a time delay in space variation (such as headway, NNRD, or analogous measures) and velocity variation in response to perturbation ( $\varepsilon$ ), performed as:

$$\delta = t(\mathbf{v}_\varepsilon) - t(\mathbf{s}_\varepsilon). \quad (1)$$

In this context,  $t(\mathbf{v}_\varepsilon)$  denotes the response moment of velocity to perturbation ( $\varepsilon$ ), while  $t(\mathbf{s}_\varepsilon)$  denotes the response moment of space to perturbation ( $\varepsilon$ ). When  $\delta > 0$  holds, we characterize the pedestrian's behavior as anticipation behavior. Conversely, when  $\delta < 0$  satisfied, we designate the pedestrian's behavior as reaction behavior.

**Swarm Factor** Here, we introduce the concept of the Swarm factor to assess the spatial dynamics of pedestrians based on sociological cognition. Hall (1966) defined four circular pedestrian space requirements, consisting of intimate distance, personal distance, social distance, and public distance, as shown in Fig. 6. An intimate space is reserved for close friends, lovers, children, and close family members. During normal daily movement, people will avoid letting strangers enter their intimate space. Therefore, from a sociological perspective, the intimate distance can be considered as the critical distance during the crossing process.

Based on the individual requirement, the swarm factor ( $S$ ) was defined to characterize the congestion level of pedestrians, with the formula:

$$S_p = \sum_q n_q(t) \quad (2)$$

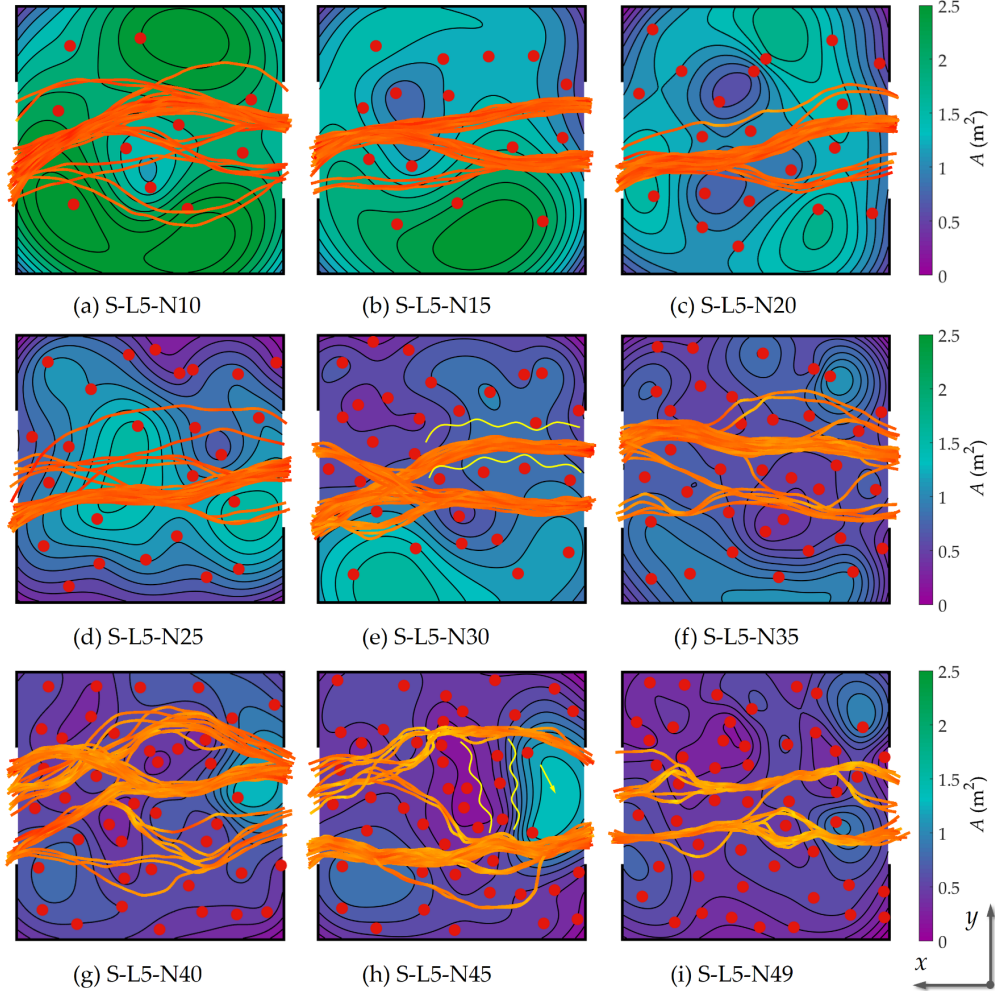


**Figure 4:** The local area field diagrams in different experiments superimposed on the trajectories (The red dots in the diagram represent the distribution of static participants and the coordinate given in the lower right corner).

$$n_q(t) = \begin{cases} 1 & \text{if } \|\mathbf{x}_q(t) - \mathbf{x}_p(t)\| < r \\ 0 & \text{otherwise} \end{cases} \quad (3)$$

Here,  $S_p$  represents the swarm factor of pedestrian  $p$  at moment  $t$ , while  $n_q(t)$  is a binary variable denotes for a given pedestrian  $q$ , whether any pedestrian  $p$  enters the intimate space at moment  $t$ .  $\mathbf{x}_q(t)$  denotes the coordinate of pedestrian  $q$  at time  $t$ , similar conventions apply to  $\mathbf{x}_p(t)$ . In this paper,  $r$  is set to be 0.4 m, which is slightly smaller than the upper limit of intimate distance. Therefore, when the swarm factor is not equal to zero, it indicates that the pedestrian is in an uncomfortable state concerning their social attributes.

#### 4.1.2. Behavioral Patterns

Fig.7 presents the swarm factor variation versus speed within the static context. The changes in pedestrian velocity show a continuous increase and decrease rather than sudden transitions. Additionally, based on measurements of the swarm factor, the amplitude of the swarm factor and speed changes are limited during the crossing process. Through the comparison of the swarm factor and velocity, there lack of distinctive features for recognising behavioral patterns. We conjecture that, when crossing through the static crowd, the variations in the environment have a limited impact on velocity. Firstly, pedestrians actively avoid high-density areas during the crossing process; moreover, the

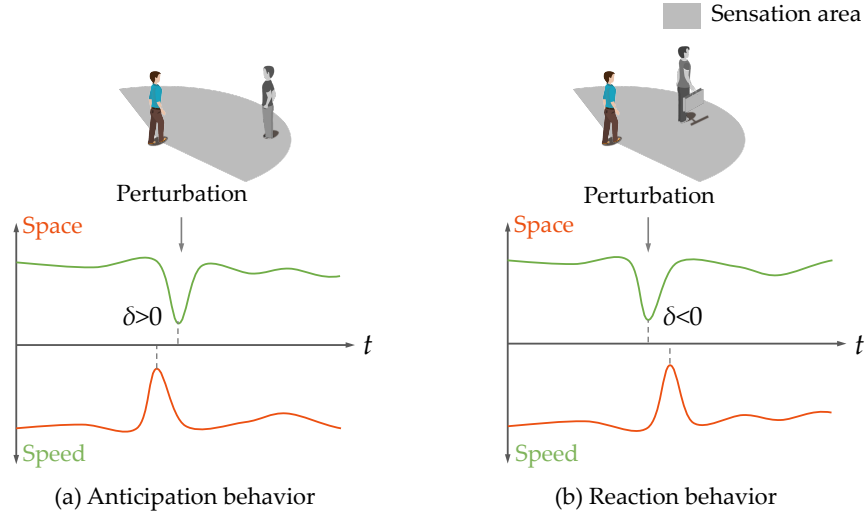


**Figure 5:** Schematic diagram of anticipation and reaction behavior during pedestrian motion (the Sensation area in the diagram changes according to the specific measurement metric).

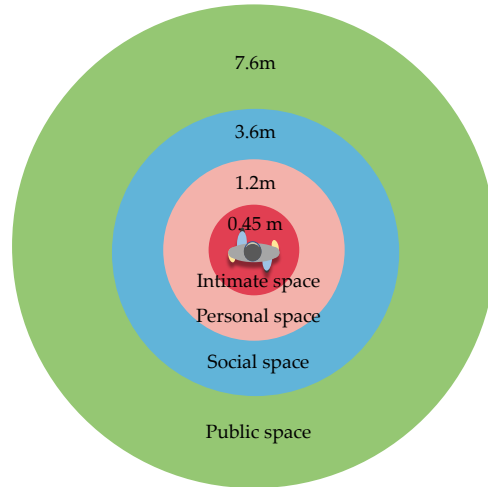


**Figure 6:** Diagram of individual space requirement (Intimate distance: close phase: below six inches, far phase: six to eighteen inches; personal space: close phase: one and a half to two and a half feet, far phase: two and a half to four feet; social distance: close phase: four to seven feet, far phase: seven to twelve feet; public space: close phase: twelve to twenty-five feet, far phase: twenty-five feet or more, Source: [Hall \(1966\)](#)).

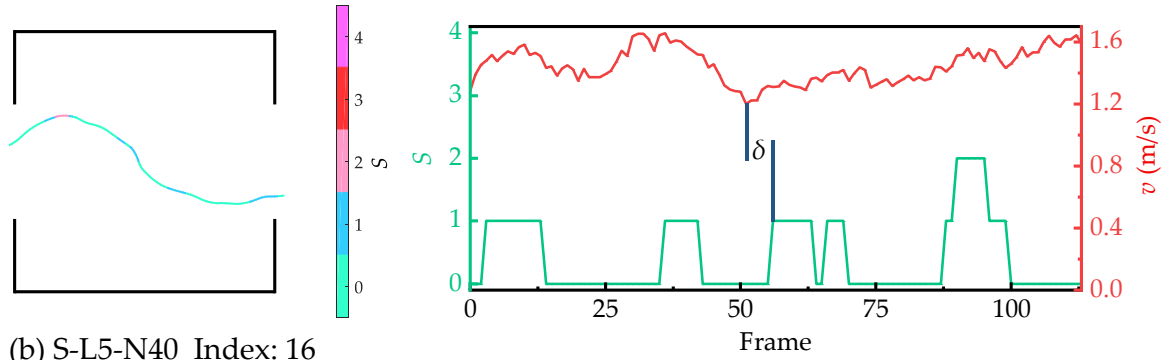
static environment allows pedestrians to plan their trajectories and be immune to potential collisions. Consequently, pedestrians can maintain streamlined trajectories.

In the dynamic context, the temporal evolution of pedestrian velocity versus the swarm factor is illustrated in Fig.8. In the figures, we marked  $\delta$  to represent TD. Compared to the variation from static experiments, we can observe that the speed and the swarm factor exhibited more sustained fluctuations. Moreover, the response of pedestrians to spatial variation is more readily discernible due to its asynchronous nature. The pre-action and post-action of pedestrian response enable the distinction between anticipation behavior and reaction behavior. Pedestrians have been observed to exhibit different behavior patterns between anticipation and reaction to adapt to the intricate dynamics within dynamic crowds, as illustrated in Fig.8.

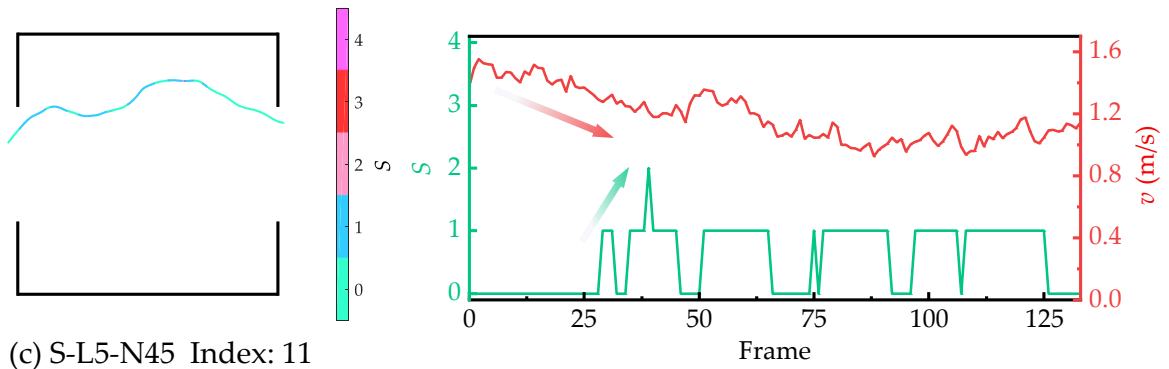
## 4.2. Velocity analysis

### 4.2.1. Crossing Efficiency

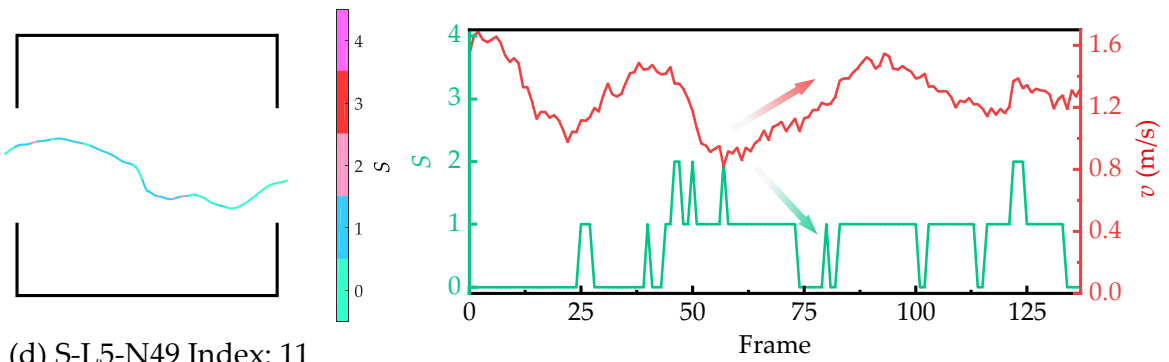
(a) S-L5-N35 Index: 9



(b) S-L5-N40 Index: 16



(c) S-L5-N45 Index: 11



(d) S-L5-N49 Index: 11

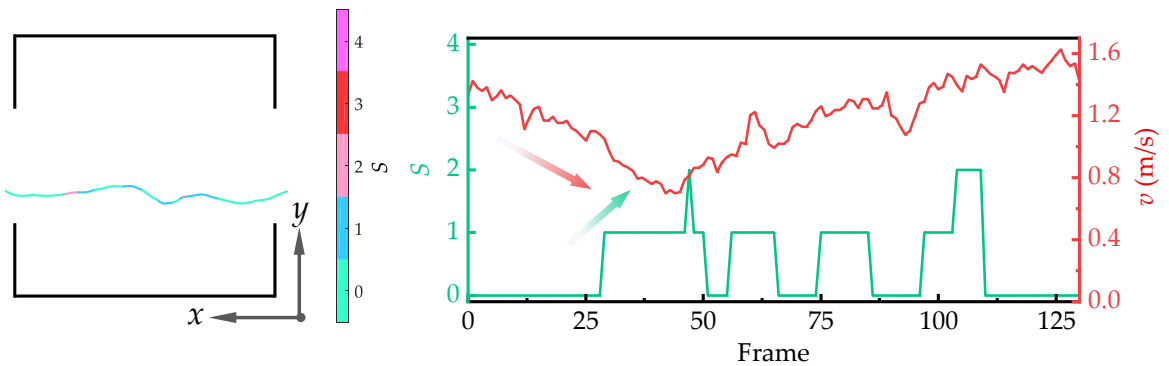
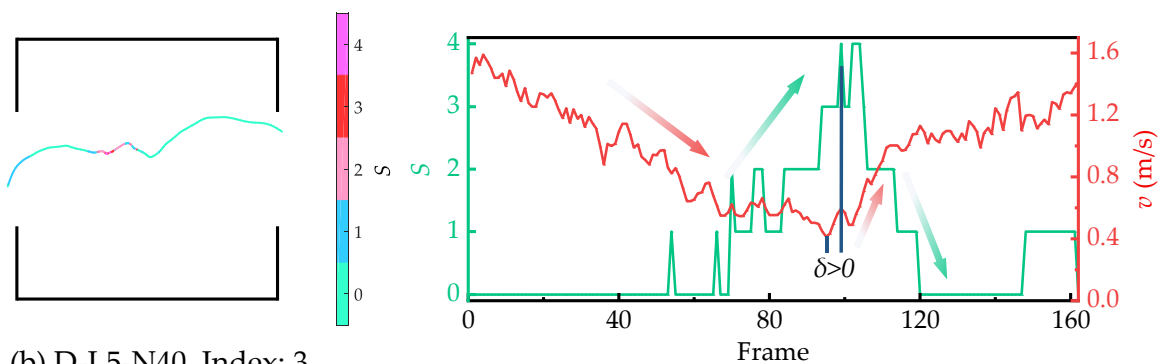
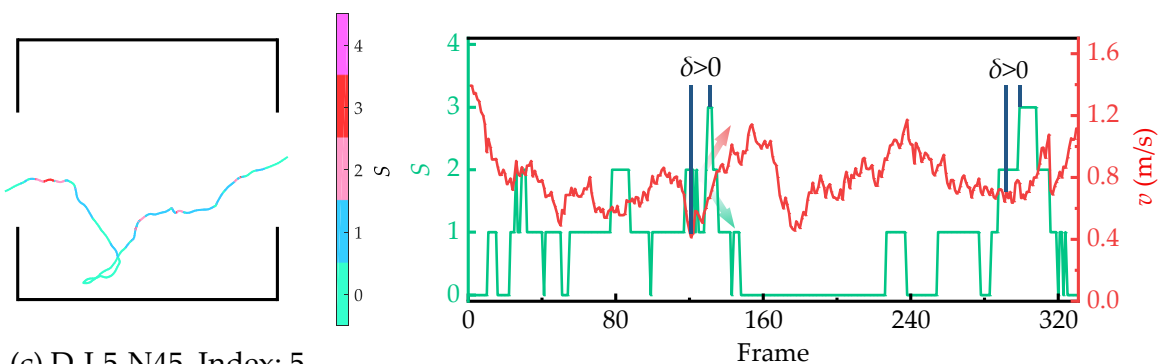


**Figure 7:** Speed variation versus swarm factor variation of cross pedestrians in static context, the subheadings indicate the selected pedestrian indexes, representing the trajectories of the respective experiments.

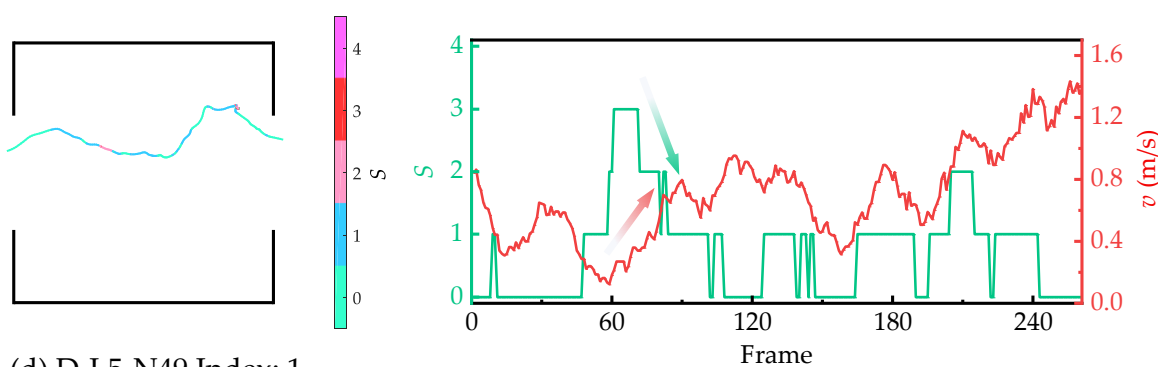
(a) D-L5-N35 Index: 34



(b) D-L5-N40 Index: 3



(c) D-L5-N45 Index: 5



(d) D-L5-N49 Index: 1

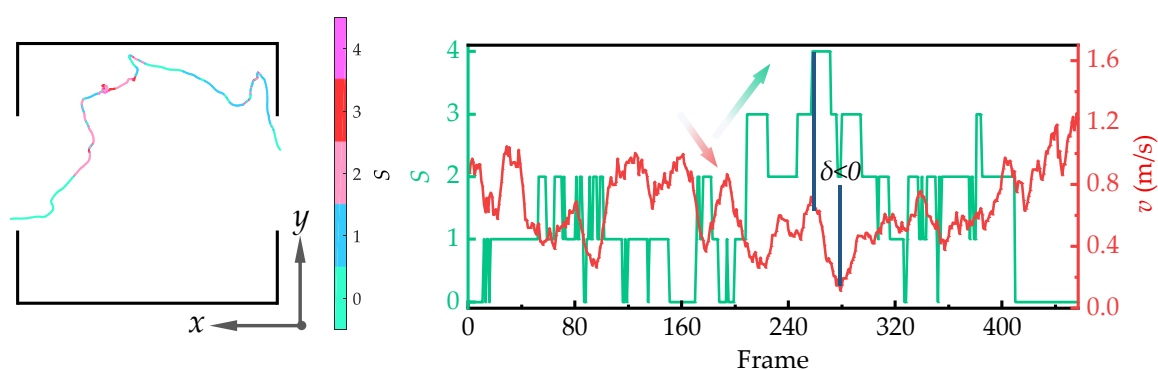


**Figure 8:** Speed variation versus swarm factor variation of cross pedestrians in the dynamic context, the subheadings indicate the selected pedestrian indexes, representing the trajectories of the respective experiments.

The average crossing speed ( $\bar{v}_x$ ) denotes the average velocity in the crossing direction within the crossing process, and serves as the measure of pedestrians' cross-efficiency within the crowd, expressed as:

$$\bar{v}_x = \frac{\int_{t_{in}}^{t_{out}} v_x dt}{t_{out} - t_{in}} = \frac{L}{t_{out} - t_{in}}. \quad (4)$$

Here,  $L$  denotes the crossing length,  $t_{in}$  indicates the moment of the pedestrian entering the experimental area, and  $t_{out}$  represents the moment of the pedestrian leaving the experimental area. The distribution of average crossing speeds under static and dynamic configurations is presented in Fig.9. It is evident that the average crossing speed of the static crowd is significantly higher than the dynamic crowd. Within the static condition, the highest speed peak is observed in experiment S-L5-N5 (mean = 1.59 m/s), whereas the dynamic condition exhibits its speed peak in experiment D-L5-N0 (mean = 1.48 m/s). As the global density increases, the disparity in average crossing speed tends to widen.

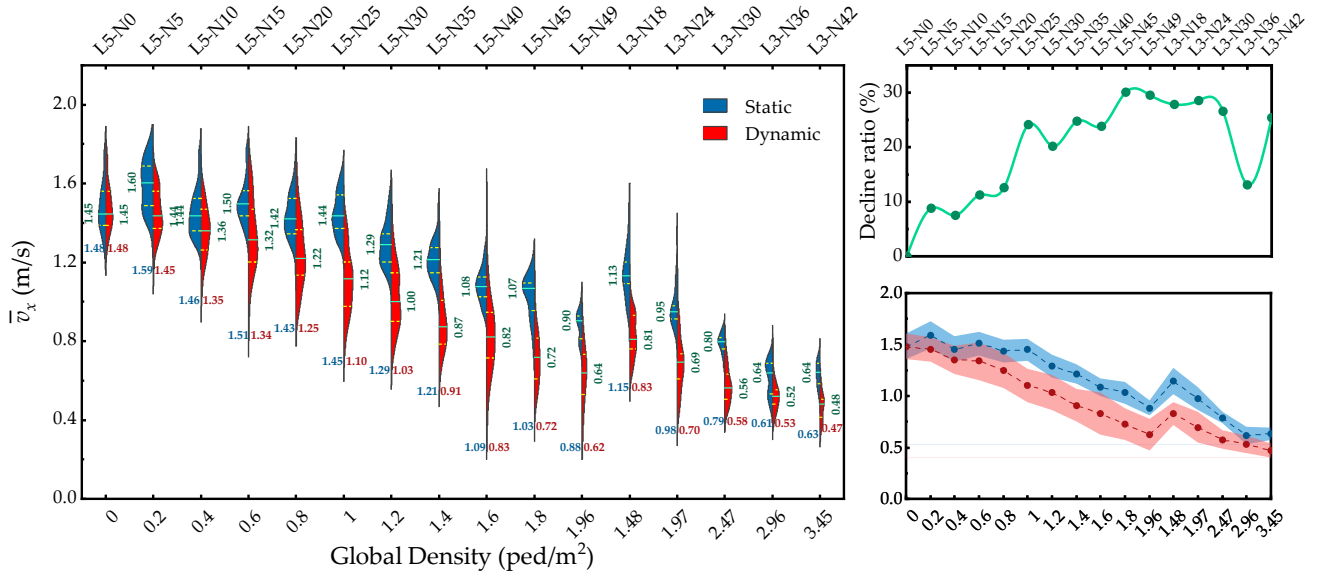


**Figure 9:** Pedestrians' average crossing speed variation in different experimental groups, with median (thick green line and green numbers), upper and lower quartiles (yellow dotted line), and mean data (red and blue numbers). The subplots reflected the trend of the speed difference in static and dynamic contexts and the variation trend of mean and standard deviation (mean  $\pm$  SD), respectively.

#### 4.2.2. Orthogonal Analysis

In this part, the pedestrians' velocity is decomposed into two orthogonal components: the crossing direction (in the  $x$ -direction) and the transverse direction (in the  $y$ -direction). This decomposition allows us to investigate the variations in crossing velocity ( $v_x$ ) and transverse velocity ( $v_y$ ) so that different detour features within static and dynamic contexts can be quantitatively elucidated. The velocity deconstruction correspondence within each experiment is independently analyzed, as illustrated in Fig.10.

Fig.10 presented a consistently linear relationship between the crossing velocity ( $v_x$ ) and the instantaneous velocity ( $v$ ). Moreover, by comparing the distribution trends at different global densities, transverse velocity ( $v_y$ ) exhibits a systematic increase within the dynamic context (L5-N5  $\sim$  L5-N49), indicating that pedestrians exhibit a higher frequency of detours.

Fig. 11 illustrates the corresponding variations in the instantaneous velocity ( $v$ ), the crossing velocity ( $v_x$ ), and the absolute value of the transverse velocity ( $|v_y|$ ). A comparison between Fig.11(a) and Fig.11(b) reveals that velocity fluctuations expand with increasing global density. Moreover, within the dynamic context, the fluctuations of the crossing velocity are more pronounced compared to the static context. Most importantly, in both dynamic and static experiments, the dynamics of pedestrians crossing exhibit a fundamental pattern: with an increase in global density,

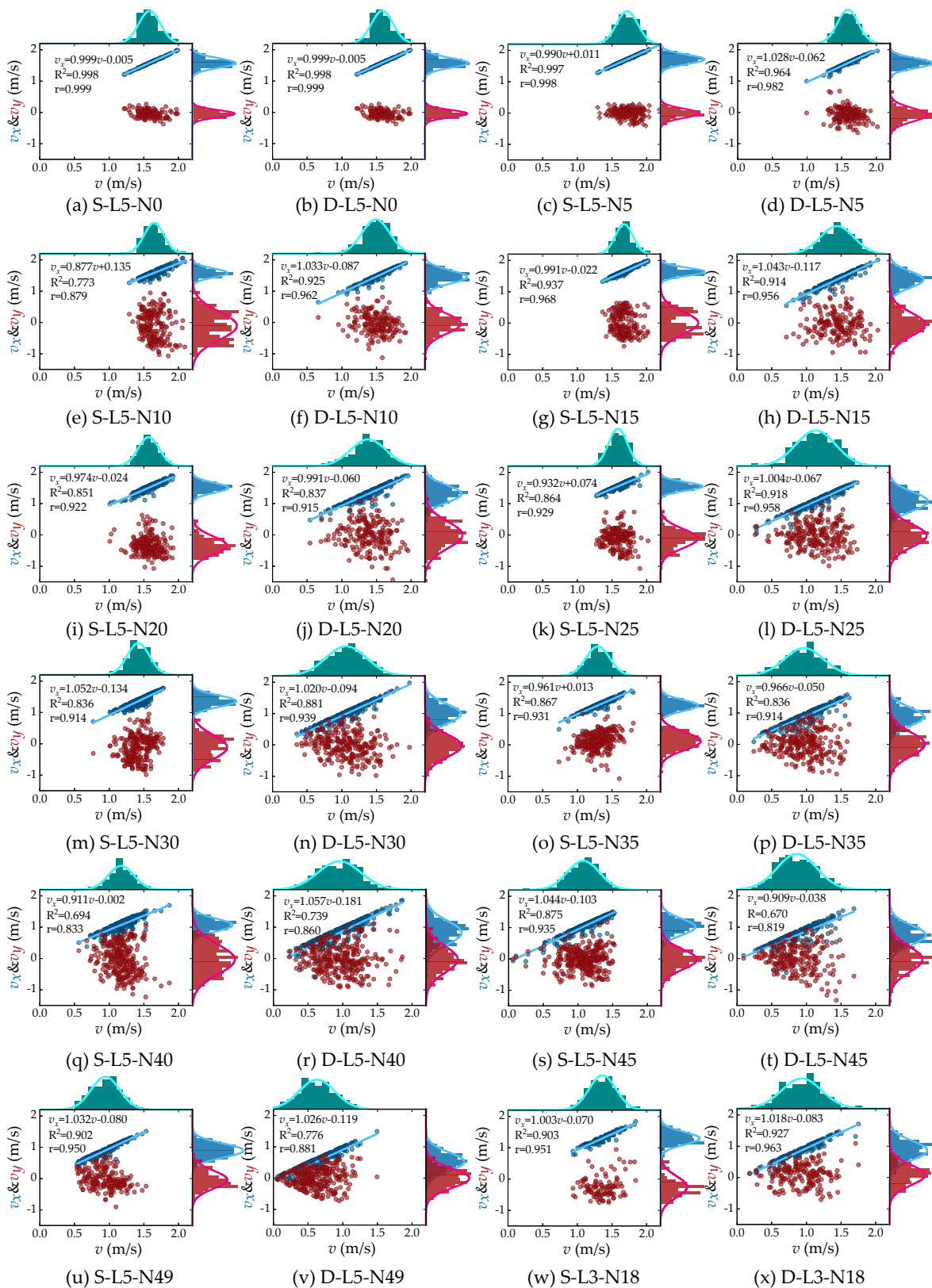


**Figure 10:** The kernel density and the associated marginal histograms of instantaneous velocities along orthogonal directions for various experiments.

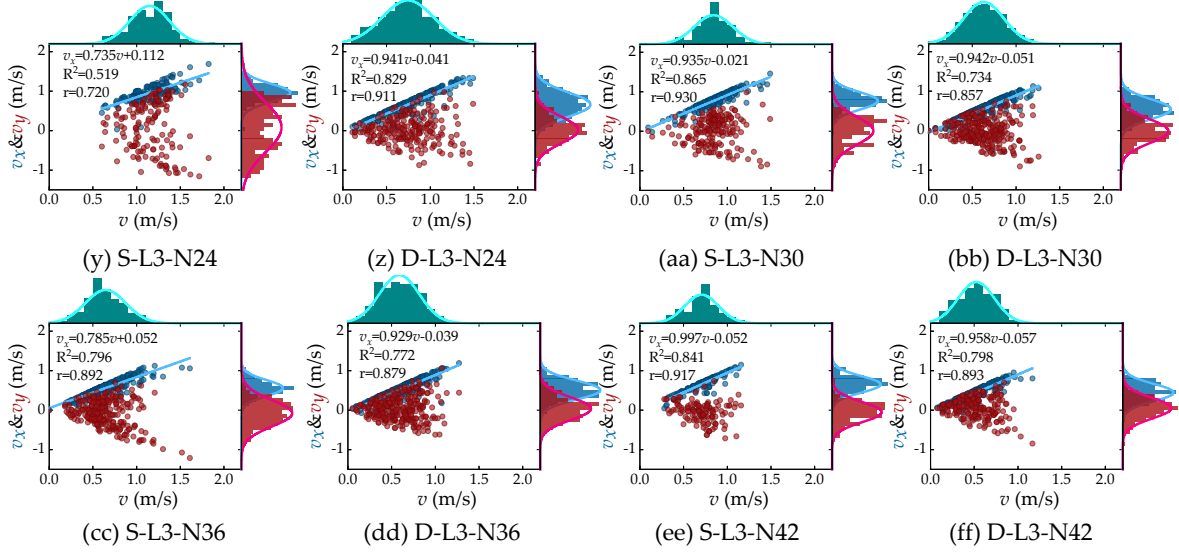


Figure 10: (continued).

the instantaneous velocity and crossing velocity decrease, while the transverse velocity remains within the interval of  $[0.2, 0.5]$ . This observation implies that even in highly congested scenarios, pedestrians will continue to strategically keep motion through detours (Wang et al. 2023).

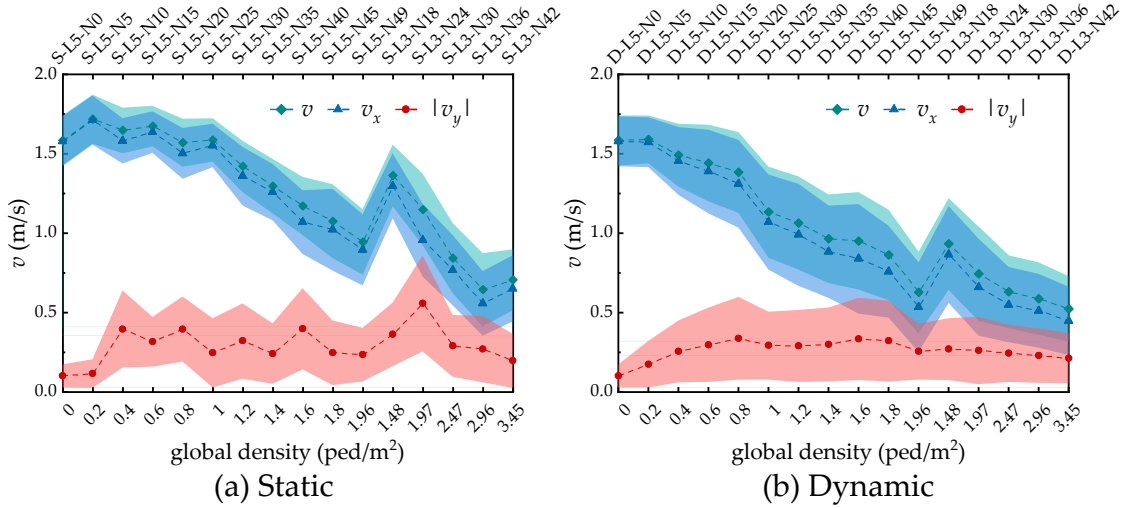


Figure 11: Relationship between instantaneous velocity and component velocity in different experimental groups. The dash and the shaded area represent the mean value and one-sigma error (mean  $\pm$  standard deviation), respectively.

## 5. CONCLUSIONS

In this paper, we investigated pedestrian crossing behavior within dynamic and static contexts. The qualitative analysis of pedestrian trajectories reveals distinct characteristics when pedestrians crossing static or dynamic crowds. The formation of cross-channels, a unique self-organization phenomenon within static crowds, has been observed.

To investigate the discrepancies in pedestrian crossing behavior, we introduced quantitative metrics to analyze the differences in motion patterns and trajectories. Within static contexts, pedestrians' speeds and swarm factors are not sensitive to the increases in global density and do not exhibit typical behavioral patterns. The similar desensitization mechanism might contribute to the formation of cross-channels. In contrast, within dynamic crowds, the speeds and swarm factors of crossing pedestrians show dramatic fluctuations and contribute to quantitatively classifying

the anticipation and reaction behaviors. Moreover, the orthogonal analysis of velocity illustrated the cross-efficiency variation induced by the crowd contexts. Fundamental patterns in pedestrian motion have been identified: with the elevation of global density, both the instantaneous and crossing velocities decrease, while transverse velocity appears unaffected. This phenomenon proves detour behavior may serve as a crucial mechanism for pedestrians to maintain dynamism within dense crowds.

This study contributes to the empirical knowledge of pedestrian behavior pattern and a deeper understanding of crowd dynamics.

#### DATA AVAILABILITY

The data can be found here: <https://doi.org/10.34735/ped.2019.4> (Pedestrian Dynamics Data Archive) or [https://drive.google.com/drive/folders/1NYVnRp0z8VPuskfezMr51gB-sraOf6Iq?usp=drive\\_link](https://drive.google.com/drive/folders/1NYVnRp0z8VPuskfezMr51gB-sraOf6Iq?usp=drive_link) (Google Drive).

#### ACKNOWLEDGMENTS

This work was supported by the National Natural Science Foundation of China (Grant No. 52072286, 71871189, 51604204), and the Fundamental Research Funds for the Central Universities (Grant No. 2022IVA108).

#### REFERENCES

- Cao, S., Seyfried, A., Zhang, J., Holl, S., & Song, W. 2017, *Journal of Statistical Mechanics: Theory and Experiment*, 2017, 033404, doi: [10.1088/1742-5468/aa620d](https://doi.org/10.1088/1742-5468/aa620d)
- Cordes, J., Chraïbi, M., Tordeux, A., & Schadschneider, A. 2023, *Crowd Dynamics, Volume 4: Analytics and Human Factors in Crowd Modeling*, 143, doi: [10.1007/978-3-031-46359-4\\_6](https://doi.org/10.1007/978-3-031-46359-4_6)
- Feliciani, C., Corbetta, A., Haghani, M., & Nishinari, K. 2023, *Safety science*, 164, 106174, doi: [10.1016/j.ssci.2023.106174](https://doi.org/10.1016/j.ssci.2023.106174)
- Feliciani, C., & Nishinari, K. 2016, *Physical Review E*, 94, 032304, doi: [10.1103/PhysRevE.94.032304](https://doi.org/10.1103/PhysRevE.94.032304)
- Hall, E. T. 1966, *The hidden dimension*, Vol. 609 (Anchor)
- Helbing, D., Johansson, A., & Al-Abideen, H. Z. 2007, *Physical review E*, 75, 046109, doi: [10.1103/PhysRevE.75.046109](https://doi.org/10.1103/PhysRevE.75.046109)
- Helbing, D., Keltsch, J., & Molnar, P. 1997, *Nature*, 388, 47, doi: [10.1038/40353](https://doi.org/10.1038/40353)
- Jin, C.-J., Jiang, R., Wong, S., et al. 2019, *Transportation research part C: emerging technologies*, 109, 137, doi: [10.1016/j.trc.2019.10.013](https://doi.org/10.1016/j.trc.2019.10.013)
- Kleinmeier, B., Köster, G., & Drury, J. 2020, *Journal of the Royal Society Interface*, 17, 20200396, doi: [10.1098/rsif.2020.0396](https://doi.org/10.1098/rsif.2020.0396)
- Ma, J., Song, W., & Lo, S. 2015, in *Traffic and Granular Flow'13*, Springer, 103–110
- Moussaïd, M., Garnier, S., Theraulaz, G., & Helbing, D. 2009, *Topics in Cognitive Science*, 1, 469, doi: [10.1111/j.1756-8765.2009.01028.x](https://doi.org/10.1111/j.1756-8765.2009.01028.x)
- Mullick, P., Fontaine, S., Appert-Rolland, C., et al. 2022, *PLoS computational biology*, 18, e1010210, doi: [10.1371/journal.pcbi.1010210](https://doi.org/10.1371/journal.pcbi.1010210)
- Murakami, H., Feliciani, C., Nishiyama, Y., & Nishinari, K. 2021, *Science Advances*, 7, eabe7758, doi: [10.1101/2020.08.09.215178](https://doi.org/10.1101/2020.08.09.215178)
- Nicolas, A., Kuperman, M., Ibañez, S., Bouzat, S., & Appert-Rolland, C. 2019, *Scientific reports*, 9, 105, doi: [10.1038/s41598-018-36711-7](https://doi.org/10.1038/s41598-018-36711-7)
- Parisi, D. R., Negri, P. A., & Bruno, L. 2016, *Physical Review E*, 94, 022318, doi: [10.1103/physreve.94.022318](https://doi.org/10.1103/physreve.94.022318)
- Portz, A., & Seyfried, A. 2011, in *Pedestrian and Evacuation Dynamics* (Springer), 577–586, doi: [10.1007/978-1-4419-9725-8\\_52](https://doi.org/10.1007/978-1-4419-9725-8_52)
- Seyfried, A., Passon, O., Steffen, B., et al. 2009, *Transportation science*, 43, 395, doi: [10.1007/978-3-540-77074-9\\_17](https://doi.org/10.1007/978-3-540-77074-9_17)
- Steffen, B., & Seyfried, A. 2010, *Physica A: Statistical mechanics and its applications*, 389, 1902, doi: [10.1016/j.physa.2009.12.015](https://doi.org/10.1016/j.physa.2009.12.015)
- Wang, J., Lv, W., & Cao, S. 2024, arXiv preprint arXiv:2401.03656
- Wang, J., Lv, W., Jiang, H., Fang, Z., & Ma, J. 2023, arXiv preprint arXiv:2311.04827
- Zanlungo, F., Feliciani, C., Yücel, Z., & Nishinari, K. 2023a, *Safety science*, 158, 105969, doi: [10.1016/j.ssci.2022.105969](https://doi.org/10.1016/j.ssci.2022.105969)
- Zanlungo, F., Feliciani, C., Yücel, Z., Nishinari, K., & Kanda, T. 2023b, *Safety science*, 158, 105953, doi: [10.1016/j.ssci.2022.105953](https://doi.org/10.1016/j.ssci.2022.105953)
- Zuriguel, I., Echeverría, I., Maza, D., et al. 2020, *Safety science*, 121, 394, doi: [10.1016/j.ssci.2019.09.014](https://doi.org/10.1016/j.ssci.2019.09.014)